MOLECULAR AND CELLULAR BIOLOGY, Dec. 1997, p. 7386–7397 Vol. 17, No. 12
0270-7306/97/$04.00+0

Adenovirus-Mediated Overexpression of IRS-1 Interacting Domains Abolishes Insulin-Stimulated Mitogenesis without Affecting Glucose Transport in 3T3-L1 Adipocytes

PREM M. SHARMA,[1] KATSUYA EGAWA,[1] THOMAS A. GUSTAFSON,[2] JODY L. MARTIN,[1] AND JERROLD M. OLEFSKY[1,3,4]*

Department of Medicine, Division of Endocrinology and Metabolism,[1] and Whittier Diabetes Institute,[3] University of California, San Diego, La Jolla, California 92093[1]; Veterans Administration Research Service, San Diego, California 92161[4]; and Department of Physiology, University of Maryland School of Medicine, Baltimore, Maryland 21201[2]

Received 2 July 1997/Returned for modification 27 August 1997/Accepted 26 September 1997

Activated insulin receptor (IR) interacts with its substrates, IRS-1, IRS-2, and Shc via the NPXY motif centered at Y960. This interaction is important for IRS-1 phosphorylation. Studies using the yeast two-hybrid system and sequence identity analysis between IRS-1 and IRS-2 have identified two putative elements, the PTB and SAIN domains, between amino acids 108 and 516 of IRS-1 that are sufficient for receptor interaction. However, their precise function in mediating insulin's bioeffects is not understood. We expressed the PTB and SAIN domains of IRS-1 in HIRcB fibroblasts and 3T3-L1 adipocytes utilizing replication-defective adenoviral infection to investigate their role in insulin signalling. In both cell types, overexpression of either the PTB or the SAIN protein caused a significant decrease in insulin-induced tyrosine phosphorylation of IRS-1 and Shc proteins, IRS-1-associated phosphatidylinositol 3-kinase (PI 3-K) enzymatic activity, $p70^{s6k}$ activation, and p44 and p42 mitogen-activated protein kinase (MAPK) phosphorylation. However, epidermal growth factor-induced Shc and MAPK phosphorylation was unaffected by the overexpressed proteins. These findings were associated with a complete inhibition of insulin-stimulated cell cycle progression. In 3T3-L1 adipocytes, PTB or SAIN expression extinguished IRS-1 phosphorylation with a corresponding 90% decrease in IRS-1-associated PI 3-K activity. $p70^{s6k}$ is a downstream target of PI 3-K, and insulin-stimulated $p70^{s6k}$ was inhibited by PTB or SAIN expression. Interestingly, overexpression of either PTB or SAIN protein did not affect insulin-induced AKT activation or insulin-stimulated 2-deoxyglucose transport, even though both of these bioeffects are inhibited by wortmannin. Thus, interference with the IRS-1–IR interaction inhibits insulin-stimulated IRS-1 and Shc phosphorylation, PI 3-K enzymatic activity, $p70^{s6k}$ activation, MAPK phosphorylation and cell cycle progression. In 3T3-L1 adipocytes, interference with the IR–IRS-1 interaction did not cause inhibition of insulin-stimulated AKT activation or glucose transport. These results indicate a bifurcation or subcompartmentalization of the insulin signalling pathway whereby some targets of PI 3-K (i.e., $p70^{s6k}$) are dependent on IRS-1-associated PI 3-K and other targets (i.e., AKT and glucose transport) are not. IR–IRS-1 interaction is not essential for insulin's effect on glucose transport, and alternate, or redundant, pathways exist in these cells.

After insulin receptor (IR) activation, multiple signalling pathways are activated leading to diverse effects upon cellular metabolism and mitogenesis. Once activated, the IR can tyrosine phosphorylate endogenous substrates, such as IR substrate 1 (IRS-1) (41, 49), IR substrate 2 (IRS-2) (42, 45), Shc (32), and others (25, 50, 52). The best-studied IR substrates are IRS-1 and the signalling adapter protein Shc. The cDNA encoding IRS-1 protein has been isolated from rats, mice, and humans (4, 28, 41, 48). IRS-1, a cytoplasmic protein of 160 to 185 kDa as indicated by sodium dodecyl sulfate-polyacrylamide gel electrophoresis (SDS-PAGE), is expressed in a broad range of tissues and is highly conserved across species. The first step in insulin signalling involves autoactivation of the receptor by phosphorylation of tyrosines 1146, 1150, and 1151 in its catalytic cleft and tyrosine 960 in its juxtamembrane region. IRS-1 phosphorylation is mediated by interaction with the NPXY motif centered at phosphotyrosine 960 of the autophosphorylated IR (4, 28, 48).

IRS-1 contains a pleckstrin homology domain at its extreme amino-terminal region, whose deletion markedly impairs Tyr phosphorylation of IRS-1 in vivo and the capability of IRS-1 to associate and activate phosphatidylinositol 3-kinase (PI 3-K) (27, 47). At the carboxyl-terminal end of the pleckstrin homology domain of the IRS-1 protein, at least two additional regions are considered necessary for efficient interaction with the activated receptor. Studies using the yeast two-hybrid system suggest that amino acids 108 to 516 of IRS-1, termed the IR binding domain (IRBD), are sufficient for binding phosphotyrosine 960 of the IR and are required for phosphorylation of IRS-1 by the IR (8, 12, 14). Deletion analysis within the IRBD of IRS-1 has further identified amino acids 313 to 462 to be essential for interaction with IR; these amino acids show a high degree of similarity with Shc amino acids 41 to 200 (3, 8, 12, 14, 18, 44). This region is termed the Shc and IRS-1 NPXY binding (SAIN) domain. Furthermore, the recent cloning of IRS-2 has revealed extensive similarity between IRS-1 and IRS-2 among amino acids 144 to 316, suggesting the existence of another minimal IRBD, termed the phosphotyrosine binding (PTB) domain (42). A PTB domain was first described as a 186-amino-acid segment in the NH_2 terminus of Shc (3, 12). However, it shares no recognizable sequence identity with the IRS-1 PTB (3, 18), although its three-dimensional structure is similar. X-ray crystal structure analyses indicate that the overall patterns of ligand binding by the IRS-1 and Shc PTB do-

* Corresponding author. Mailing address: Department of Medicine (0673), University of California, San Diego, 9500 Gilman Dr., La Jolla, CA 92093-0673. Phone: (619) 534-6651. Fax: (619) 534-6653.

mains are similar, but residues critical for phosphotyrosine recognition are not conserved (10).

Once IRS-1 is tyrosine phosphorylated, it can serve as a docking protein for a number of SH2 domain-containing signalling proteins, such as the 85-kDa regulatory subunit of phosphatidylinositol 3-kinase (PI 3-K). This p85 subunit binds to specific phosphotyrosine motifs of IRS-1 leading to activation of PI 3-K and stimulation of downstream PI 3-K-mediated signalling events.

Abundant evidence from *Xenopus* oocytes, cell culture systems, single-cell microinjection studies, and animal models (4, 28, 48) has demonstrated the central role of IRS-1 in mediating downstream effects of insulin and insulin-like growth factor 1 (IGF-1). Phosphorylation of IRS-1 has been shown to be necessary for normal insulin-mediated cell cycle progression in a variety of cell systems (17, 35). In contrast, the role of IRS-1 in the regulation of classic metabolic responses to insulin is less clear. Reducing IRS-1 expression in rat adipose cells by using an antisense ribozyme leads to modest impairment of insulin-stimulated glucose transporter translocation, and disruption of the IRS-1 gene in mice causes reduced intra-uterine growth, elevated fasting insulin levels, and only mild insulin resistance. These data suggest that IRS-1 plays a role in glucose homeostasis, although other pathways must be involved (48). A recent report from our laboratory suggests that phosphorylated IRS-1 is not an essential component of the metabolic insulin signalling pathway that leads to GLUT4 translocation in 3T3-L1 adipocytes (26). Thus, the role of IRS-1 in the regulation of classic metabolic responses to insulin remains unclear, in part because convenient experimental systems for investigating this role are unavailable.

To investigate the role of IRS-1 in distinct mitogenic and metabolic responses to insulin, we have utilized replication-defective adenoviral-mediated infection of rapidly dividing fibroblasts and differentiated 3T3-L1 adipocytes, along with a variety of biochemical assays. These cells were transiently infected with recombinant adenoviral constructs expressing the PTB (amino acids 144 to 316) and SAIN (amino acids 313 to 462) domains of IRS-1 in order to investigate their role in insulin signalling.

MATERIALS AND METHODS

Materials. Porcine insulin was kindly provided by Lilly. Mouse monoclonal antiphosphotyrosine (PY-20), mouse monoclonal anti-ERK1, rabbit polyclonal insulin receptor β, and anti-Shc-SH2 antibodies were purchased from Transduction Laboratories. Anti-IRS-1 and anti-human S6 kinase ($p70^{s6k}$) were from Upstate Biotechnology Incorporated. Phospho-specific MAPK and $p70^{s6k}$ antibodies were from New England Biolabs, Inc. The goat polyclonal AKT (C-20) and the rabbit polyclonal insulin receptor β (C-19) antibodies of human origin were purchased from Santa Cruz Biotechnology. Horseradish peroxidase-linked anti-rabbit, -mouse, and -goat antibodies were obtained from Amersham. Dulbecco's modified Eagle's medium (DMEM) and fetal bovine serum (FBS) were obtained from Life Technologies. Restriction enzymes and a random primer DNA labelling kit were purchased from Bethesda Research Laboratories (Gaithersburg, Md.). All radioisotopes were obtained from DuPont-NEN (Boston, Mass.). Hoechst dye 33342 was obtained from Molecular Probes (Eugene, Oreg.). XAR-5 film was obtained from Eastman Kodak (Rochester, N.Y.). All other reagents and chemicals were purchased from Sigma.

Cell culture. Rat 1 fibroblasts that had been stably transfected and that overexpress wild-type human insulin receptor (HIRcB cells) were cultured as described previously (17). 3T3-L1 cells were grown and maintained in high-glucose DMEM containing 50 U of penicillin/ml, 50 μg of streptomycin/ml, and 10% FBS in a 10% CO_2 environment. The cells were allowed to grow for 2 days postconfluency and were then differentiated by addition of the same medium containing isobutylmethylxanthine (500 μM), dexamethasone (25 μM), and insulin (4 μg/ml) for 3 days and then by addition of the medium containing insulin for 3 additional days. The medium was then changed every 3 days until the cells were fully differentiated, which typically occurred by the 10th day. Prior to experimentation, the adipocytes were trypsinized and reseeded in the appropriate culture dishes. The Ad-E1A-transformed human embryonic kidney cell line 293 was cultured in DMEM containing 10% FBS.

Plasmid construction. The PTB and SAIN domains of human IRS-1 were amplified by PCR using Pfu polymerase (Boehringer Mannheim, France) with different sets of the following primers (5′ to 3′): ctagtctaga**gccgccaccatg**GGCA GCTCCGGCCTTGGTGAGGCT (primer 1), gcccaagcttTCAGCCTGGCTTC CCGCCCACCATGCT (primer 2), ctagtctaga**gccgccaccatg**GCCACCTCCCCG GCCAGCATG (primer 3), and gcccaagcttTCAGGGCCCCTTGCCACCCAT GCA (primer 4). *Xba*I and *Hin*dIII, the 5′ and the 3′ cloning sites, respectively, are underlined. The PCR products containing PTB or SAIN domains of IRS-1 were digested with *Xba*I and *Hin*dIII and were cloned into *Xba*I- and *Hin*dIII-digested pACCMVpLpA (vector containing an ampicillin selection marker) and digested with *Xba*I and *Hin*dIII. Kozak sequences including a methionine initiation codon (indicated in bold letters) were inserted upstream of the 5′ end of the PCR primers. The inserted fragments were in frame with the initiation codon. The plasmids pAC-PTB and pAC-SAIN, obtained by cloning the cDNA fragments, were amplified with the primer sets 1-2 and 3-4. They encode the PTB and SAIN domain-specific proteins containing amino acids 144 to 316 and 313 to 462, respectively of the IRS-1 protein. The nucleotide sequences of the cloned plasmids were verified by DNA sequence analysis using the 5′- and the 3′-end specific primers around the cloning sites (*Xba*I and *Hin*dIII) of the plasmid, pACCMVpLpA.

Preparation of recombinant adenovirus. The recombinant adenoviruses containing the cDNA encoding the PTB and SAIN domains of human IRS-1 were isolated by homologous recombination with two plasmids, pACCMVpLpA (11) and pJM17 (24), by following the strategy summarized in Fig. 1A. The recombinant plasmids, pAC-PTB, pAC-SAIN, and pJM17, were purified and cotransfected into 293 cells. Since 293 cells were originally derived from adenovirus transformation, the missing E1 gene function of pJM17 is provided in *trans*. The resulting recombinant viruses containing the PTB and SAIN domains of human IRS-1 are denoted Ad5-PTB and Ad5-SAIN, respectively, and are replication defective (at least in cells lacking the E1 region of adenovirus) but fully infectious.

Detection of recombinant Ad5-PTB and Ad5-SAIN or wild-type virus in cell culture medium by PCR amplification of viral DNA. DNA templates for PCR were extracted from the supernatant of the culture medium (350 μl) of the 293 cells that were infected with each plaque isolate or virus at a multiplicity of infection (MOI) of 50 PFU/ml. A multiplex PCR was performed on a 1/10 dilution of virus DNA using E1A and E2B region-specific primers (51), and the products were analyzed for the presence of recombinant or wild-type adenovirus. The presence of PTB and SAIN domain-specific cDNA inserts of human IRS-1 in the recombinant virus was confirmed by PCR analysis of viral DNA with IRS-1 cDNA-specific primers. One clone of each of the recombinant viruses was amplified further in 293 cells. Purification by cesium chloride centrifugation resulted in higher titer stocks of the recombinant viruses, typically 10^{10} PFU/ml as determined by limiting dilution. All recombinant adenoviruses were stored at −70°C in phosphate-buffered saline containing 10% glycerol.

Cell treatment. HIRcB cells were transduced at a multiplicity of infection of 1 to 20 PFU/cell for 1 h with stocks of either a negative control recombinant adenovirus (Ad5-Ctrl or Ad5-CMV) containing the cytomegalovirus promoter, pUC 18 polylinker, and a fragment of the simian virus 40 genome or the recombinant adenoviruses Ad5-PTB and Ad5-SAIN. 3T3-L1 adipocytes required either 10-fold more virus or a longer infection time (12 to 16 h) than HIRcB cells to achieve >90% infection in a transient system. Transduced cells were incubated for 48 to 72 h at 37°C in 5% CO_2 and DMEM with 2% heat-inactivated serum in order to minimize cell division and to avoid a hormonal effect on gene expression and/or on the activities of overexpressed proteins, followed by incubation in the starvation medium required for the assay. The experiments were performed 60 to 96 h after the viral incubation and were repeated three to five times. The efficiency of adenovirus-mediated gene transfer was approximately 90% as measured by histocytochemical staining for β-galactosidase (β-Gal) of the cells infected with the recombinant adenovirus Ad5-lacZ, containing the bacterial β-Gal gene (data not shown). The survival of the differentiated 3T3-L1 adipocytes was unaffected by incubation of cells with the different adenovirus constructs since the total cell protein remained the same in infected or uninfected cells. However, the HIRcB cells demonstrated about 10% decrease in total cellular protein, thereby indicating inhibition of cell cycle progression.

RNA extraction and Northern blot analysis. Total RNA was isolated from control (uninfected) and Ad5-PTB and Ad5-SAIN domain-expressing adenovirus-infected cells as described elsewhere (38). Total RNA (15 μg) was denatured and electrophoresed on a 1% agarose–6.6% formaldehyde gel and blotted onto a Hybond-N^+ membrane. A 586-bp cDNA fragment of human IRS-1 spanning the PTB and SAIN domains was labelled with [α-^{32}P]dCTP by random priming. Northern blots were hybridized with the labelled probe and washed as described previously (38). Ethidium bromide staining of the electrophoresed RNA was used to visualize the loading pattern. The autoradiograph was obtained after a 6-h exposure and was analyzed with a Hewlett-Packard Scan Jet II P desk scanner utilizing a scan analysis program.

DNA synthesis. Cells were infected with the indicated adenoviruses at increasing MOIs (0.2, 2.0, 20) for 1 h at room temperature, serum starved for 36 h, and then stimulated with insulin (100 ng/ml) in the presence of BrdU for 16 h at 37°C. They were then fixed and processed for immunofluorescence by sequential incubation with rat anti-BrdU antibody and rhodamine-conjugated donkey anti-rat antibody. Cells were counterstained with Hoechst stain to visualize nuclei. BrdU-

incorporated cells were identified by the nuclear rhodamine staining (red). An average of 200 cells per coverslip were counted. Results are expressed as the percentages of stained cells exhibiting nuclear fluorescence.

PI 3-K activity. In vitro phosphorylation of PI was carried out in immune complexes as described previously (36). Cells were infected with Ad5-PTB or Ad5-SAIN or with Ad5-CMV or Ad5-lacZ at the indicated MOIs and times and were grown in medium containing heat-inactivated serum (2%) for 48 h. Serum-starved (16 h) cells were incubated in the absence (basal) or presence of insulin (100 ng/ml) for 30 min, washed once with ice-cold phosphate-buffered saline, lysed, and subjected to immunoprecipitation (400 to 500 μg total protein) with antibodies to IRS-1 or IR-β (2 to 4 μg), overnight at 4°C. Immune complexes were precipitated from the supernatant with protein A-Sepharose (Sigma) and washed as previously described (36). The washed immune complexes were incubated with PI (Avanti) and [γ-^{32}P]ATP (3,000 Ci/mmol) for 10 min at room temperature. Reactions were stopped with 20 μl of 8 N HCl and 160 μl of $CHCl_3$-methanol (1:1) and centrifuged, and the lower organic phase was removed and applied to a silica gel thin-layer chromatography plate (Merck) which had been coated with 1% potassium oxalate. Thin-layer chromatography plates were developed in $CHCl_3$-CH_3OH-H_2O-NH_4OH (60:47:11.3:2) and dried, and immune complexes were visualized and quantitated on a Molecular Dynamics PhosphorImager.

2-Deoxyglucose transport. The procedure for assessing glucose transport was a modification of the methods described by Klip et al. (19). Differentiated 3T3-L1 adipocytes were infected with Ad5-PTB or Ad5-SAIN (or Ad5-lacZ or Ad5-CMV) at the indicated MOIs for 12 to 16 h at 37°C and grown in medium containing heat-inactivated serum (2%) for 48 h. Serum- and glucose-deprived cells were incubated in α-MEM in the absence (basal) or presence of 100 ng of insulin/ml for 1 h at 37°C. In another set of experiments, cells were incubated with 1, 10, or 100 ng of insulin/ml for 1 h at 37°C. Glucose uptake was determined in duplicate at each point after the addition of 10 μl of substrate ([2-^{3}H]deoxyglucose or L-[^{3}H]glucose; 0.1 μCi; final concentration, 0.01 mmol/liter) to provide a concentration at which cell membrane transport is rate limiting. The value for L-glucose was subtracted to correct each sample for the contributions of diffusion and trapping. Data are representative of three different observations, and each value was corrected for protein content.

Immunoprecipitation and Western blotting. HIRcB cells and 3T3-L1 adipocytes, either uninfected or infected with Ad5-PTB, Ad5-SAIN, Ad5-CMV, or Ad5-lacZ, were starved for 24 h in serum-free Cellgro medium. The cells were stimulated with insulin (100 ng/ml or as indicated in the figure legends) for 5 to 30 min at 37°C and lysed in a solubilizing buffer containing 30 mM Tris, 150 mM EDTA, 1% Nonidet P-40, 0.5% sodium deoxycholate, 0.1% SDS, and 1 mM Na_3VO_4 (pH 7.4) for 20 min at 4°C. The cell lysates were centrifuged to remove insoluble materials. For Western blot analysis, whole-cell lysates (60 to 80 μg of protein per lane) from the indicated cells were denatured by boiling in Laemmli sample buffer containing 100 mM dithiothreitol and resolved by SDS-PAGE. Gels were transferred to Immobilon-P membranes by electroblotting in Towbin buffer containing 0.02% SDS and 20% methanol and were immunoblotted with the indicated antibody. For immunoprecipitations, the supernatants (400 to 500 μg of protein) were immunoprecipitated with anti-Shc antibody (1:100 dilution) overnight at 4°C. The entire precipitant and all of the remaining supernatant proteins were then separated by SDS–7.5% PAGE and transferred to Immobilon-P membranes by electroblotting. For immunoblotting, membranes were blocked and probed with specified antibodies. Blots were then incubated with a second horseradish peroxidase-linked antibody followed by chemiluminescence detection according to the manufacturer's instructions (Pierce).

RESULTS

Detection of recombinant Ad5-PTB and Ad5-SAIN or wild-type virus by multiplex PCR analysis. We employed a multiplex PCR assay to detect trace amounts of wild-type adenovirus in a given batch of recombinant viruses. For this approach, we designed two pairs of primers for the same reaction that can amplify E1A DNA and E2B DNA (an internal control). Recombinant viruses, Ad5-PTB and Ad5-SAIN, and the controls, Ad5-lacZ and Ad5-CMV, were isolated as outlined in the legend for Fig. 1A and described in Materials and Methods. Purified viruses with genotypes of E1 deletion (Ad5-CMV/Ad5-Ctrl,), E1 substitution (Ad5-lacZ, Ad5-PTB, and Ad5-SAIN), or the wild type were selected for detection of recombinant or wild-type viruses by multiplex PCR. Culture medium from 293 cells that had been infected with plaque isolates or virus at an MOI of 50 PFU/ml and exhibited cytopathic effects was used as the source of template DNA. Multiplex PCR amplification of the viral DNA was performed with E1A and E2B specific primers. The E1A DNA (indicative of wild-type virus) was not detected from any plaque-purified recombinant Ad5-lacZ, Ad5-PTB, and Ad5-SAIN but was specifically detected when the DNA template from the wild-type virus-infected cell culture was used as a template (data not shown). These results indicate that the recombinants were free of wild-type virus contamination. E2B PCR-positive clones indicate the presence of adenovirus (wild type or recombinant). To further confirm the presence of recombinant cDNAs in E2B PCR-positive clones, the Ad5-PTB and Ad5-SAIN virus DNAs were PCR amplified with specific primers derived from the Ad5 polylinker (5′ and 3′ of the cloning site) and with the cDNA-specific primers 1-2 and 3-4, respectively (see Materials and Methods). cDNA fragments of 519 and 450 bp were detected from the PTB and SAIN domain clones, respectively, indicating the presence of recombinant DNA. No PCR product was detected in the wild-type virus-infected cell culture DNA (data not shown).

Determination of transfection efficiency and Northern blot analysis of overexpressed PTB and SAIN mRNAs isolated from infected cells. To assess infection efficiency, we used immunohistochemistry techniques to examine the expression of recombinant adenovirus containing a nuclear-localizing variant of the bacterial β-Gal gene, Ad5-lacZ, following infection of HIRcB fibroblasts and 3T3-L1 adipocytes at MOIs of 1 to 100 PFU/cell. The infection efficiency was assessed by determining the percentage of cells expressing Ad5-lacZ. Ad5-lacZ also served as a control for the effect of adenovirus per se on infected cells. In three independent experiments, >90% of the HIRcB cells and 3T3-L1 adipocytes showed positive immunostaining at ~20 to 50 PFU/cell on postinfection day 3, as judged by the number of blue nuclei per 200 cells, while untreated cells exhibited no blue color in the presence of the β-Gal chromogenic substrate (data not shown). Infection with Ad5-lacZ or Ad5-CMV resulted in no apparent differences in the morphological features of HIRcB cells and 3T3-L1 adipocytes, including the extent of adipocyte differentiation and the number of differentiated adipocytes compared with untreated cells on postinfection days 3 to 5.

Northern blot analysis was used to confirm the expression of PTB and SAIN mRNAs in HIRcB cells following infection with increasing MOIs (2, 8, 20, and 80 PFU/cell) of Ad5-PTB and Ad5-SAIN adenoviruses. Similarly, mRNA levels were detected in 293 cells (cells used for isolation of the recombinant adenoviruses) infected at an MOI of 1 PFU/cell. As shown in Fig. 1B, a dose-dependent increase in mRNA expression of the PTB and SAIN domains of human IRS-1 was observed in HIRcB (lanes 2 to 5) and 293 (lane 7) cells but was absent in the noninfected cells (lanes 1 and 6). To further compare the levels of PTB and SAIN mRNA expression in HIRcB fibroblasts and 3T3-L1 adipocytes, both the cell lines were infected at the same MOIs (5 and 20 PFU/cell) of Ad5-PTB- and Ad5-SAIN-expressing adenoviruses and total RNA was isolated after 3 days postinfection. Results of Northern blot analysis (Fig. 1C) confirmed that the two cell lines express similar levels of PTB and SAIN mRNAs. Densitometric scanning of the blot revealed that treatment of the cells resulted in a 20- to 100-fold increase in mRNA levels relative to the uninfected cells. Due to unavailability of specific antibodies for the PTB and SAIN domains, Western blot analysis could not be performed.

Studies of HIRcB fibroblasts. (i) Inhibition of insulin-stimulated IRS-1 phosphorylation. In theory, the IRS-1-derived PTB and SAIN domains should competitively inhibit the interaction between endogenous IRS-1 and the IR β-subunit juxtamembrane domain, resulting in decreased IRS-1 phosphorylation. To assess this, whole-cell lysates from insulin-treated HIRcB fibroblasts overexpressing PTB and SAIN pro-

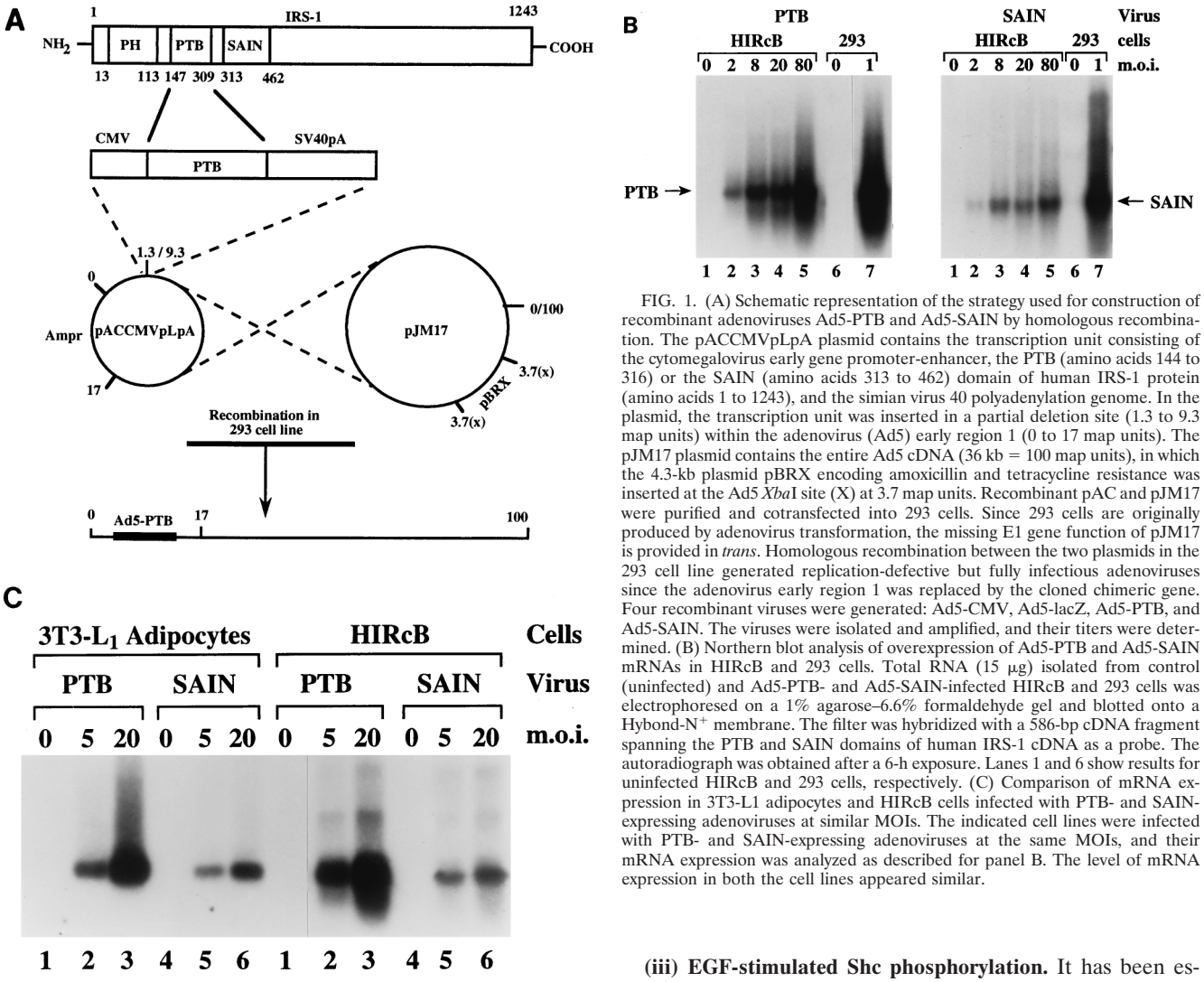

FIG. 1. (A) Schematic representation of the strategy used for construction of recombinant adenoviruses Ad5-PTB and Ad5-SAIN by homologous recombination. The pACCMVpLpA plasmid contains the transcription unit consisting of the cytomegalovirus early gene promoter-enhancer, the PTB (amino acids 144 to 316) or the SAIN (amino acids 313 to 462) domain of human IRS-1 protein (amino acids 1 to 1243), and the simian virus 40 polyadenylation genome. In the plasmid, the transcription unit was inserted in a partial deletion site (1.3 to 9.3 map units) within the adenovirus (Ad5) early region 1 (0 to 17 map units). The pJM17 plasmid contains the entire Ad5 cDNA (36 kb = 100 map units), in which the 4.3-kb plasmid pBRX encoding amoxicillin and tetracycline resistance was inserted at the Ad5 *Xba*I site (X) at 3.7 map units. Recombinant pAC and pJM17 were purified and cotransfected into 293 cells. Since 293 cells are originally produced by adenovirus transformation, the missing E1 gene function of pJM17 is provided in *trans*. Homologous recombination between the two plasmids in the 293 cell line generated replication-defective but fully infectious adenoviruses since the adenovirus early region 1 was replaced by the cloned chimeric gene. Four recombinant viruses were generated: Ad5-CMV, Ad5-lacZ, Ad5-PTB, and Ad5-SAIN. The viruses were isolated and amplified, and their titers were determined. (B) Northern blot analysis of overexpression of Ad5-PTB and Ad5-SAIN mRNAs in HIRcB and 293 cells. Total RNA (15 μg) isolated from control (uninfected) and Ad5-PTB- and Ad5-SAIN-infected HIRcB and 293 cells was electrophoresed on a 1% agarose–6.6% formaldehyde gel and blotted onto a Hybond-N^+ membrane. The filter was hybridized with a 586-bp cDNA fragment spanning the PTB and SAIN domains of human IRS-1 cDNA as a probe. The autoradiograph was obtained after a 6-h exposure. Lanes 1 and 6 show results for uninfected HIRcB and 293 cells, respectively. (C) Comparison of mRNA expression in 3T3-L1 adipocytes and HIRcB cells infected with PTB- and SAIN-expressing adenoviruses at similar MOIs. The indicated cell lines were infected with PTB- and SAIN-expressing adenoviruses at the same MOIs, and their mRNA expression was analyzed as described for panel B. The level of mRNA expression in both the cell lines appeared similar.

teins were subjected to SDS-PAGE and immunoblotted with anti-phosphotyrosine monoclonal antibody. The 180- to 190-kDa IRS-1 protein was strongly phosphorylated in response to insulin in uninfected and control-infected (Ad5-CMV) HIRcB fibroblasts (Fig. 2A, lanes 2 to 4). However, the Ad5-PTB- and Ad5-SAIN-infected cells exhibited an 80 to 90% inhibition of IRS-1 tyrosine phosphorylation with no effect on insulin receptor β-subunit tyrosine phosphorylation (Fig. 2A, lanes 5 to 8).

(ii) Inhibition of insulin-stimulated Shc phosphorylation. Shc is another PTB domain-containing substrate which becomes tyrosine phosphorylated after interaction with the IR juxtamembrane domain (32, 37). Because both Shc and IRS-1 interact with the IR juxtamembrane region, we determined whether overexpression of the IRS-1 PTB and SAIN domains could affect insulin-stimulated Shc phosphorylation. Cell lysates from insulin-treated cells were immunoprecipitated with anti-Shc antibody and immunoblotted with antiphosphotyrosine antibody. A four- to fivefold increase in insulin-stimulated tyrosine phosphorylation of p52 Shc was observed in uninfected and Ad5-CMV-infected cells (Fig. 2B, lanes 2 to 3), and this was completely inhibited by overexpression of the PTB and SAIN domains (Fig. 2B, lanes 4 to 7).

(iii) EGF-stimulated Shc phosphorylation. It has been established that epidermal growth factor (EGF) induces tyrosine phosphorylation of p52 and p46 isoforms of the Shc protein. We determined whether overexpression of the IRS-1 PTB and SAIN domains could affect EGF-stimulated Shc phosphorylation. Cell lysates from EGF-treated cells were immunoprecipitated with anti-Shc antibody and immunoblotted with antiphosphotyrosine antibody. An 8- to 10-fold increase in EGF-stimulated tyrosine phosphorylation of p52 and p46 isoforms of the Shc protein was observed in uninfected cells (Fig. 2C, lane 2), and this was not affected significantly by overexpression of either the PTB or SAIN domain (Fig. 2C, lanes 3 to 6). Consistent with our previous results, these data indicate that EGF-directed Shc phosphorylation primarily involves the Shc SH2 domain (37) and demonstrate the selectivity of IRS-1 PTB or SAIN overexpression for insulin signalling events.

(iv) IRS-1-associated PI 3-K activity. It is well established that tyrosine-phosphorylated IRS-1 associates with and activates PI 3-K (4, 28, 48). Therefore, we measured IRS-1-associated PI 3-K activity in PTB, SAIN, and LacZ overexpressing HIRcB cells. In control cells, insulin stimulation resulted in a 25- to 30-fold increase in IRS-1-associated PI 3-K activity in anti-IRS-1 immunoprecipitates (Fig. 3A and B), and this effect was unchanged in Ad5-lacZ cells. Overexpression of increasing amounts of the PTB and SAIN domains led to a dose-dependent inhibition of IRS-1-associated PI 3-K activity. These re-

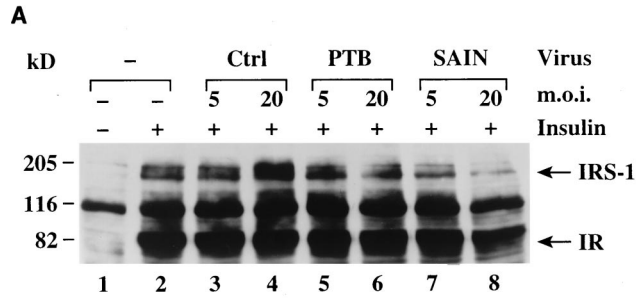

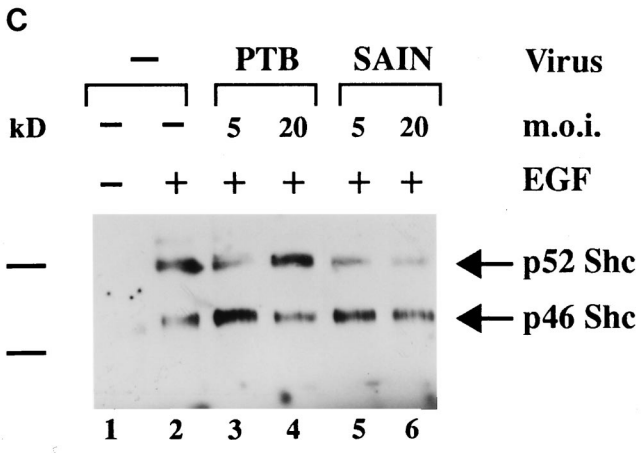

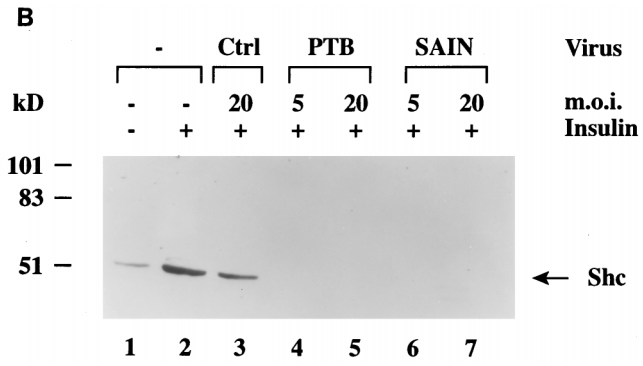

FIG. 2. (A) Effects of PTB and SAIN proteins on insulin-stimulated tyrosine phosphorylation. Whole-cell lysates (80 μg of protein per lane) from uninfected, and Ad5-CMV (Ctrl)-, Ad5-PTB-, and Ad5-SAIN-infected HIRcB cells were subjected to SDS-PAGE and immunoblotted with antiphosphotyrosine monoclonal antibody. A 5-min insulin (20 ng/ml) treatment stimulated IR β-subunit and IRS-1 phosphorylation. A significant inhibition of phosphorylation of the 180- to 190-kDa IRS-1 protein was observed. The experiment was repeated several times with appropriate controls. (B) Effects of PTB and SAIN proteins on insulin-stimulated Shc phosphorylation. HIRcB cells were infected with Ad5-PTB, Ad5-SAIN, and Ad5-CMV (Ctrl) adenoviruses for 1 h at room temperature and grown in medium containing heat-inactivated serum (2%) for 48 h. Following infection, the cells were serum starved (16 h), incubated in the absence (basal) or presence of insulin (20 ng/ml) for 5 min, lysed, and subjected to immunoprecipitation (500 μg of protein) with antibodies to Shc (5 μg). The washed immunoprecipitates were subjected to SDS-PAGE and immunoblotted with horseradish peroxidase-conjugated anti-phosphotyrosine monoclonal antibody (PY20H). Insulin stimulated p52 Shc phosphorylation. Overexpression of both the PTB and SAIN domains of IRS-1 completely inhibited insulin-stimulated phosphorylation of p52 Shc protein. (C) Effects of PTB and SAIN proteins on EGF-stimulated Shc phosphorylation. HIRcB cells were infected with Ad5-PTB and Ad5-SAIN adenoviruses for 1 h at room temperature and grown in medium containing heat-inactivated serum (2%) for 48 h. Following infection, the cells were serum starved (16 h) and were incubated in the absence (basal) or presence of EGF (100 ng/ml) for 5 min. Whole-cell lysates were subjected to immunoprecipitation (500 μg of protein) with antibodies to Shc (5 μg). The washed immunoprecipitates were subjected to SDS-PAGE and immunoblotted with antiphosphotyrosine monoclonal antibody. EGF stimulated p52 and p46 Shc phosphorylation. Overexpression of either the PTB or the SAIN domain of IRS-1 did not have a significant effect on EGF-stimulated phosphorylation of p52 and p46 Shc proteins. Markers on the left indicate 53 (top) and 35 (bottom) kDA.

sults are consistent with the finding that insulin-stimulated IRS-1 phosphorylation is inhibited in PTB- and SAIN-overexpressing cells.

(v) Insulin-stimulated activation of $p70^{s6k}$ and mitogen-activated protein kinase (MAPK). $p70^{s6k}$ is activated by multisite serine and threonine phosphorylation, which can be detected by retarded migration of the enzyme on SDS-PAGE (6); only the most highly phosphorylated forms of $p70^{s6k}$ (the slowest migrating) display increased kinase activity (6). As shown in Fig. 4A, lane 2, stimulation of HIRcB cells with insulin resulted in complete activation of $p70^{s6k}$, which was inhibited by pretreatment with 20 nM rapamycin for 30 min prior to insulin stimulation (Fig. 4A, lane 3). The PTB- and SAIN-overexpressing cells demonstrate 60 and 90% inhibition of insulin-induced $p70^{s6k}$ activation, respectively (Fig. 4A, lanes 4 to 7).

Activation of the MAPK cascade was assessed by performing Western blotting of cell lysates with a phosphospecific MAPK antibody. This antibody detects the tyrosine-phosphorylated (position 204) activated form of p44 and p42 (Erk1 and Erk2) MAPK. PTB and SAIN domains were overexpressed in HIRcB cells for 48 h, following which cells were starved for 18 h and stimulated with 100 ng of insulin/ml for 5 min. In uninfected cells, insulin stimulated phosphorylation of MAPK by about 20-fold (Fig. 4B, lane 2). Overexpression of either the PTB or SAIN domain led to a dose-dependent inhibition of MAPK phosphorylation and activation (Fig. 4B, lanes 3 to 6).

(vi) EGF-stimulated activation of MAPK. EGF-induced activation of MAPK was also assessed by Western blotting with the phosphospecific MAPK antibody. As seen in Fig. 4C, lane 5, EGF increased MAPK activation in cytosol from control adenovirus-infected HIRcB fibroblasts in 5 min by about 20-fold. Overexpression of either the PTB or SAIN domain did not alter MAPK phosphorylation in response to EGF stimulation (Fig. 4C, lanes 1 to 4). Expression of MAPK as assessed by Western blotting with a polyclonal MAPK antiserum that recognizes both nonphosphorylated and phosphorylated forms was not altered by either the PTB or SAIN domain-expressing adenovirus (data not shown). These data indicate that the PTB and SAIN domains of IRS-1 do not interfere with EGF-mediated signalling, consistent with the lack of interference of these domains with EGF-stimulated Shc phosphorylation (Fig. 2C).

(vii) Effects of PTB and SAIN domains on insulin-stimulated DNA synthesis. To evaluate a more distal biological effect, insulin-stimulated cell cycle progression was measured by monitoring BrdU incorporation into newly synthesized DNA. Cells were plated on coverslips and infected with Ad5-PTB, Ad5-SAIN, and Ad5-CMV at MOIs of 0.2, 2.0, and 20 PFU/cell, serum starved for 36 h, and then stimulated with insulin. As seen in Fig. 5A and B, 60% of the uninfected cells underwent DNA synthesis in response to insulin, and this response was not altered by Ad5-CMV infection. In contrast, overexpression of either the PTB or SAIN domain markedly inhibited insulin-stimulated DNA synthesis in a dose-dependent fashion. In addition to inhibition of DNA synthesis, these cells also displayed morphological differences. Uninfected and Ad5-CMV-infected HIRcB cells had a normal fibroblastic appear-

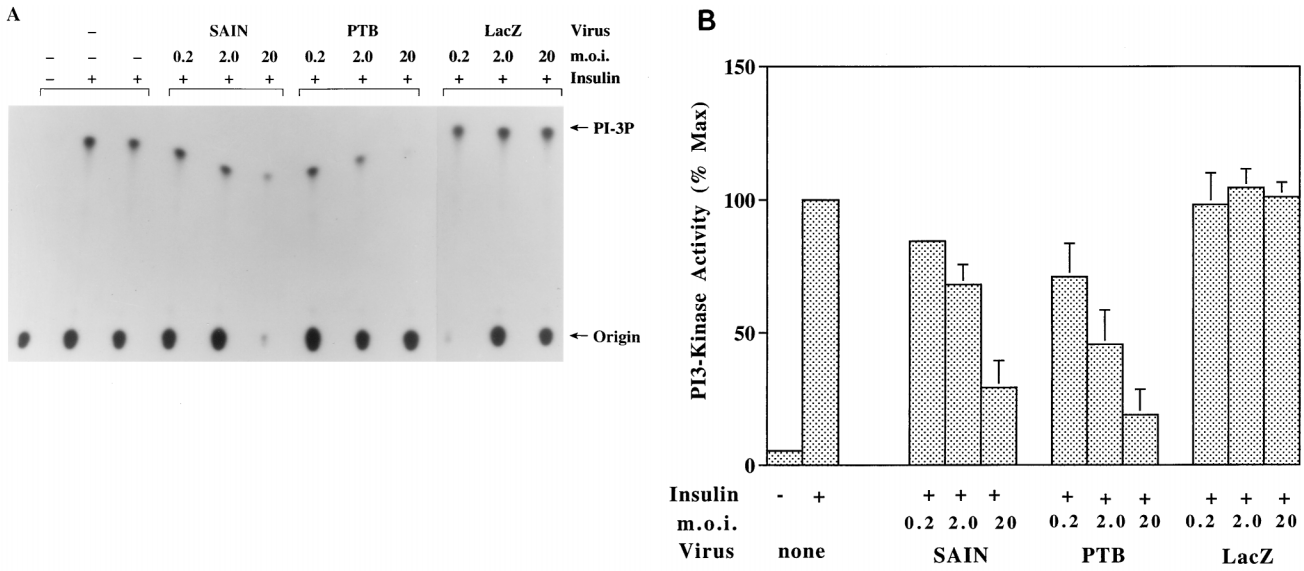

FIG. 3. Effects of overexpression of the Ad5-PTB and Ad5-SAIN domains on insulin-stimulated PI 3-K activity in HIRcB cells. Cells were infected with Ad5-PTB, Ad5-SAIN, and Ad5-lacZ for 1 h at room temperature and grown in medium containing heat-inactivated serum (2%) for 48 h. Following infection, the cells were serum starved (16 h), incubated in the absence (basal) or presence of insulin (100 ng/ml) for 30 min, lysed, and subjected to immunoprecipitation with antibodies to IRS-1. The washed immunoprecipitates were assayed for PI 3-K activity with PI as substrate, and the labeled PI 3-phosphate product (PI-3P) was resolved by thin-layer chromatography and visualized by autoradiography. (A) Data from a representative experiment; (B) means ± standard errors of the means of three experiments, expressed as percentages of the maximal activity observed in insulin-stimulated, uninfected HIRcB cells.

ance, whereas PTB- and SAIN-overexpressing cells were substantially more refractile with a more rounded shape (data not shown). These results show that when overexpressed, PTB and SAIN domains behave in a dominant-negative fashion with respect to insulin-stimulated mitogenesis.

Studies of 3T3-L1 adipocytes. (i) Effects of PTB and SAIN domains on IRS-1 phosphorylation and PI 3-K activation. A major metabolic action of insulin is stimulation of glucose transport, and 3T3-L1 adipocytes provide an excellent in vitro model system to study this biologic effect. As illustrated in Fig. 1C, these cells can be readily infected with adenoviral vectors, allowing us to study the effects of PTB and SAIN domain expression in these cells. As shown in Fig. 6, lanes 3 to 6, overexpression of the PTB or SAIN domain led to a marked inhibition of insulin-induced IRS-1 phosphorylation, as determined by antiphosphotyrosine immunoblotting of cell lysates. These same cells also demonstrated a corresponding decrease in insulin-stimulated IRS-1-associated PI 3-K activity (Fig. 7). Thus, in control cells insulin led to a seven- to eightfold increase in IRS-1-associated PI 3-kinase activity, which was markedly inhibited by expression of either the PTB or SAIN domain. In contrast, infection of the 3T3-L1 adipocytes with Ad5-CMV was without effect.

PI 3-K activity was also measured in IR immunoprecipitates from lysates of cells overexpressing the PTB and SAIN domains in response to insulin. A small fraction of PI 3-K activity was observed in IR immunoprecipitates (approximately 1 to 2% of IRS-1-associated activity), which was further stimulated by about threefold upon insulin treatment. Overexpression of PTB and/or SAIN proteins led to an ~twofold increase in IR-associated PI 3-K activity (data not shown).

(ii) Insulin-stimulated activation of MAPK. Activation of the MAPK cascade was assessed by performing Western blotting of cell lysates with a phosphospecific MAPK antibody as described above. PTB and SAIN domains were overexpressed in 3T3-L1 adipocytes for 48 h, following which cells were starved for 18 h and stimulated with 100 ng of insulin/ml for 5 min. In uninfected cells, insulin stimulated phosphorylation of MAPK by about 20-fold (Fig. 8A, lane 2). Overexpression of both the PTB and SAIN domains led to a dose-dependent inhibition of both p44 and p42 MAPK phosphorylation and activation (Fig. 8A, lanes 3 to 6). Expression of MAPK was assessed by Western blotting with a polyclonal MAPK antiserum that recognizes both nonphosphorylated and phosphorylated forms, and protein levels were not altered by infection with either the PTB or SAIN domain-expressing adenovirus (Fig. 8B, lanes 1 to 6).

(iii) Insulin-stimulated activation of $p70^{s6k}$ and AKT. The activation of $p70^{s6k}$ was determined by Western blot analysis of whole-cell lysates with a phosphospecific $p70^{s6k}$ antibody that detects $p70^{s6k}$ only when phosphorylated at Thr 421 and/or Ser 424 and does not cross-react with other phosphorylated protein kinases. 3T3-L1 adipocytes were infected with the PTB or SAIN domain-expressing adenovirus for 48 h, following which cells were starved for 18 h and stimulated with 100 ng of insulin/ml for 30 min. As shown in Fig. 9A, lane 2, stimulation of 3T3-L1 adipocytes with insulin resulted in complete activation of p70S6K, which was inhibited by pretreatment with 20 nM rapamycin for 30 min prior to insulin stimulation (Fig. 9A, lane 1). The PTB- and SAIN-overexpressing cells demonstrated 60 to 70% inhibition of insulin-induced $p70^{s6k}$ activation (Fig. 9A, lanes 4 to 7). Similar results were obtained when the membrane was stripped and reblotted with $p70^{s6k}$ antibody that detects its activation by retarded migration of the enzyme on SDS-PAGE; only the most highly phosphorylated forms of $p70^{s6k}$ (the slowest migrating) displayed increased $p70^{s6k}$ activation. As shown in Fig. 9B, lane 2, stimulation of cells with insulin resulted in activation of $p70^{s6k}$, which was blocked by PTB and SAIN proteins (Fig. 9B, lanes 4 to 7).

AKT, a serine-threonine kinase, is activated upon insulin stimulation (20), and we assessed the degree of AKT activation from the whole-cell lysates derived from insulin-stimulated 3T3-L1 cells. Insulin stimulation of 3T3-L1 adipocytes resulted in a marked stimulation of AKT activation, as determined by

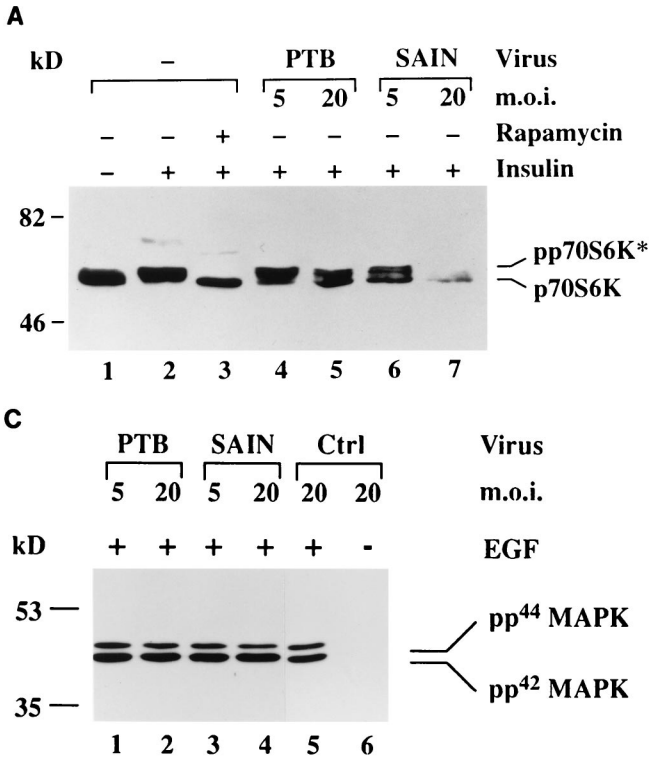

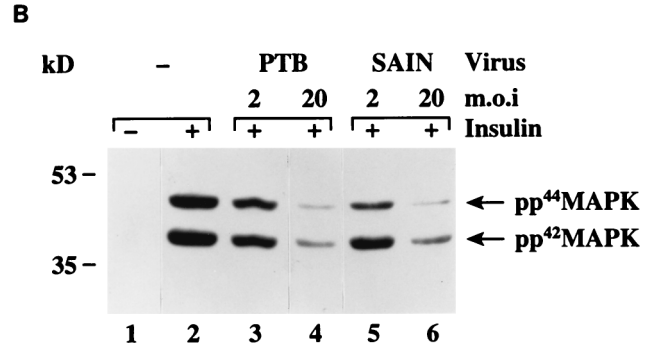

FIG. 4. (A) Effects of overexpression of the Ad5-PTB and Ad5-SAIN domains on insulin-stimulated $p70^{s6k}$ activation in HIRcB cells. Cells were infected with Ad5-PTB and Ad5-SAIN for 1 h at room temperature and grown in medium containing heat-inactivated serum (2%) for 72 h. Serum-starved (16 h) cells were incubated in the absence (basal) or presence of insulin (20 ng/ml) for 30 min, lysed, subjected to SDS-PAGE, and immunoblotted with $p70^{s6k}$ antibody. Insulin stimulation of serine and threonine phosphorylation of $p70^{s6k}$ was detected by retarded migration of the enzyme (lane 2). Preincubation with 20 nM rapamycin for 30 min inhibited activation of $p70^{s6k}$ (lane 3). Similarly, overexpression of PTB and SAIN proteins inhibited $p70^{s6k}$ activation in a dose-dependent manner (lanes 4 to 7). This experiment was repeated twice. $pp70^{s6k}$*, phosphorylated form of $p70^{s6k}$. (B) Effects of overexpression of the Ad5-PTB and Ad5-SAIN domains on insulin-stimulated MAPK phosphorylation in HIRcB cells. Cells were infected with Ad5-PTB- and Ad5-SAIN at the indicated MOIs and were treated as described for panel A except 100 ng of insulin/ml was used and cell lysates were immunoblotted with phosphospecific MAPK antibody. Insulin stimulated phosphorylation of both p44 and p42 MAPK as indicated (pp^{44} MAPK and pp^{42} MAPK, respectively). Phosphorylation of both kinases was inhibited by overexpression of PTB and SAIN proteins in a dose-dependent manner. This experiment was repeated twice. (C) Effects of overexpression of the Ad5-PTB and Ad5-SAIN domains on EGF-stimulated MAPK phosphorylation in HIRcB cells. Cells were infected with Ad5-PTB- and Ad5-SAIN-expressing adenoviruses at the indicated MOIs and treated as described for panel A except EGF (100 ng/ml) was used and cell lysates were immunoblotted with phosphospecific MAPK antibody. This experiment was repeated twice.

retarded migration of the enzyme on SDS-PAGE gel (Fig. 9C, lane 2). Interestingly, overexpression of the PTB or the SAIN proteins did not affect AKT activation, despite the fact that PI 3-K activity and $p70^{s6k}$ activation were inhibited in the same cell lysates (Fig. 9C, lanes 4 to 5 and 7 to 8, respectively). Additionally, pretreatment of cells with wortmannin, a PI 3-K inhibitor, completely blocked AKT activation (Fig. 9C, lanes 3, 6, and 9), indicating that AKT is downstream of PI 3-K. These findings suggest a bifurcation in the insulin signalling pathway such that IRS-1-associated PI 3-K activity is necessary for insulin stimulation of $p70^{s6k}$, whereas PI 3-K, but not necessarily IRS-1-associated PI 3-K, is important for AKT activation.

(iv) Insulin-stimulated glucose transport. Several reports have shown that activation of PI 3-K is both necessary and sufficient for insulin-mediated glucose transport, and phosphorylation of IRS-1 provides an important mechanism for insulin stimulation of PI 3-K. Since expression of the PTB and SAIN domains in 3T3-L1 cells inhibits IRS-1 phosphorylation and IRS-1-associated PI 3-K activity, we evaluated the effects of these domains on stimulation of glucose transport. Thus, cells were infected with Ad5-PTB, Ad5-SAIN, or Ad5-lacZ, and 2-deoxyglucose (2-DOG) uptake was measured 48 h later. As seen in Fig. 10A, insulin led to an eightfold increase in 2-DOG uptake, and this was not affected by Ad5-lacZ infection. Surprisingly, overexpression of either the PTB or the SAIN domain at MOIs of 10 and 50 was also without effect on insulin-stimulated 2-DOG uptake despite the inhibition of IRS-1 phosphorylation and IRS-1-associated PI 3-K activation in these cells (Fig. 6 and 7). To further evaluate this, a separate set of experiments was performed in which insulin dose-response studies were carried out with control cells and with PTB- SAIN- and Ad5-CMV-infected cells. As summarized in Fig. 10B, insulin-mediated glucose transport was not inhibited by infection of the cells with Ad5-CMV or with PTB or SAIN domain-carrying adenoviral vectors.

DISCUSSION

Transgenic expression of various cDNAs in tissue usually requires the preparation and isolation of stable cell lines expressing cDNAs of interest. In addition to the time required to generate these stable cell lines, there are several concerns over clonal selection and compensatory cell context changes that may occur during isolation. To circumvent these difficulties, we have utilized adenovirus-mediated gene transfer procedures for transient expression of proteins in rapidly dividing and in quiescent cells so that high levels of gene expression can be achieved and multiple functional assays can be performed. Infection of fibroblasts and 3T3-L1 adipocytes with *lacZ*-containing adenovirus resulted in the expression of β-Gal activity in >90% of the cells. Adenovirus-mediated gene transfer provides a direct means of determining whether an endogenous signalling molecule is required for a particular hormone action. In the current study, we have used this approach to overexpress the IRS-1-derived PTB and SAIN domain proteins in HIRcB cells and in 3T3-L1 adipocytes.

It is known that IRS-1 interacts with the juxtamembrane domain of the IR through its PTB and SAIN domains located in the IRS-1 NH_2 terminus. This interaction mediates IRS-1 phosphorylation, allowing it to serve as a docking protein for SH2-containing molecules, facilitating downstream signalling.

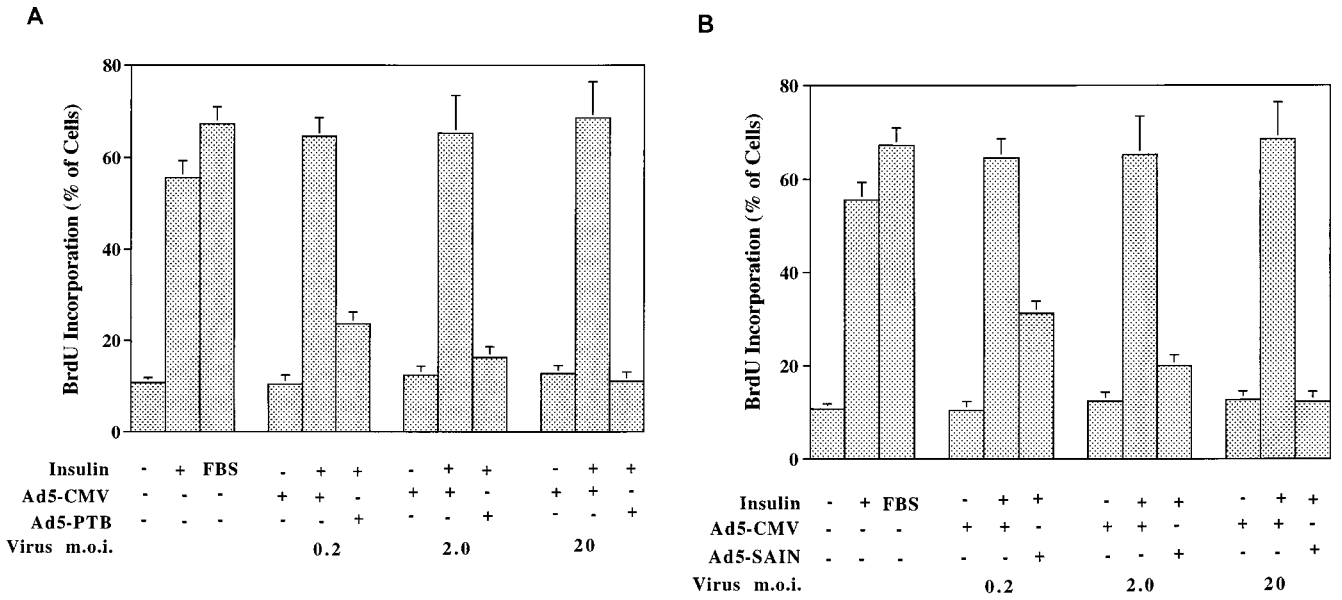

FIG. 5. Inhibition of DNA synthesis by overexpression of PTB or SAIN protein following infection of HIRcB cells with Ad5-PTB or Ad5-SAIN. Cells were infected for 1 h at room temperature with the Ad5-PTB (A) or Ad5-SAIN (B) adenoviruses at increasing MOIs as indicated, serum starved for 36 h and stimulated with insulin (100 ng/ml) in the presence of BrdU for 16 h at 37°C. They were then fixed and processed for immunofluorescence by sequential incubation with rat anti-BrdU antibody and rhodamine-conjugated donkey anti-rat antibody. Cells were counterstained with Hoechst stain to visualize nuclei. BrdU-incorporated cells were identified by the nuclear red rhodamine staining. An average of 200 cells per coverslip were counted. Results are expressed as the percentages of stained cells exhibiting nuclear fluorescence. Results presented are means ± standard errors of the means of three experiments.

The overexpressed PTB and SAIN domains should behave as competitive inhibitors of IRS-1–IR interactions, thus interfering with signalling processes mediated by endogenous IRS-1. Indeed, our data show marked inhibition of insulin-stimulated IRS-1 phosphorylation in cells overexpressing either the PTB or SAIN domain. This was associated with a corresponding decrease in insulin-stimulated IRS-1-associated PI 3-K activity as well as decreased $p70^{s6k}$ stimulation. These findings demonstrate that the inhibition of IRS-1 phosphorylation was functionally significant.

Shc is another major substrate of the IR which also interacts with the IR through a PTB domain (16). The PTB domain of Shc is similar in length and function to that in IRS-1, and both bind to the NPXY motif in the IR (3, 8, 12, 18). Interestingly, we found that overexpression of either the IRS-1 PTB or SAIN domain led to complete inhibition of insulin-induced Shc phosphorylation. Although this might seem somewhat surprising given the sequence differences between the Shc and IRS-1 PTB domains (3, 18), recent findings show that both PTB domains recognize overlapping sequences within the IR juxtamembrane region (3, 8, 12, 14, 18, 44). Therefore, it seems quite probable that the IRS-1-derived PTB and SAIN domains bind to the IRS-1 recognition motif in the IR juxtamembrane region, which, by steric hindrance, prevents access of either endogenous IRS-1 or Shc to the IR.

While we find that overexpression of the PTB or SAIN domain inhibits insulin-stimulated Shc phosphorylation and MAPK activation, it does not impair EGF-stimulated Shc phosphorylation or activation of MAPK. This would indicate that the interaction between the activated EGF receptor and Shc is primarily mediated through the SH2 domain, and this is consistent with our previous findings, obtained using the microinjection approach, on this subject (37). These results also demonstrate the selectivity of IRS-1 PTB or SAIN overexpression for insulin signalling events. We (37) and others (30, 33, 39, 40) have shown that Shc is the major substrate connecting the IR to the ras-MAPK pathway, and therefore, the blockade of Shc phosphorylation in the PTB- or SAIN-expressing cells explains the inhibition of insulin-stimulated p44 and p42 MAPK activity. Since both the ras-MAPK and IRS-1–PI 3-K pathways are necessary for insulin-induced cell cycle progression, the marked inhibition of insulin's effect to stimulate DNA synthesis in the PTB and SAIN domain-expressing cells is readily explained by the inhibition of both IRS-1 and Shc phosphorylation.

Perhaps the most novel finding from these studies relates to the lack of effect of PTB or SAIN domain expression on AKT

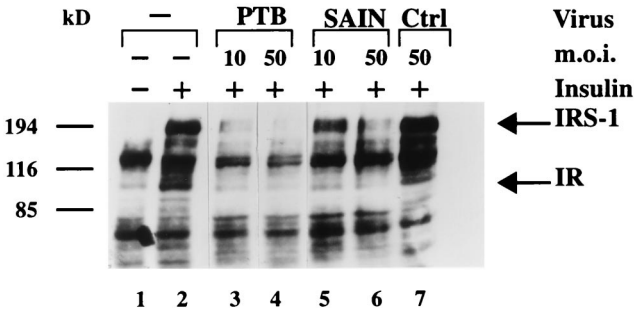

FIG. 6. Effects of overexpressed PTB and SAIN proteins in 3T3-L1 adipocytes on insulin-stimulated tyrosine phosphorylation. Whole-cell lysates (80 μg of protein per lane) from the uninfected and Ad5-PTB-, Ad5-SAIN-, and Ad5-CMV (Ctrl)-infected differentiated 3T3-L1 adipocytes were subjected to SDS-PAGE and immunoblotted with antiphosphotyrosine monoclonal antibody. A 5-min insulin (50 ng/ml) treatment stimulated IRS-1 phosphorylation (lane 2). A significant inhibition of phosphorylation of the 180- to 190-kDa IRS-1 protein was observed in 3T3-L1 adipocytes overexpressing PTB and SAIN proteins (lanes 3 to 6). The experiment was repeated several times with appropriate controls.

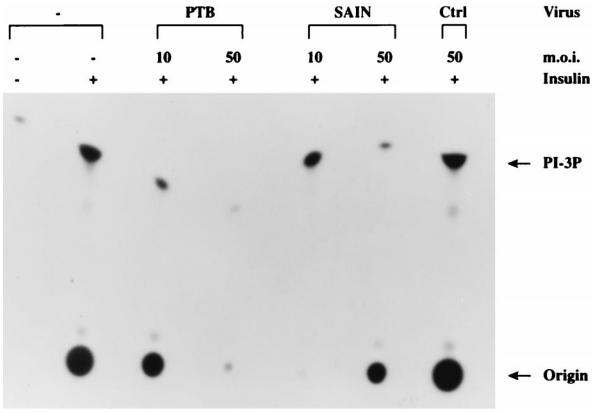

FIG. 7. Effects of overexpression of the PTB and SAIN proteins on IRS-1-associated PI 3-K activity in response to insulin in 3T3-L1 adipocytes. Cells were infected with Ad5-PTB, Ad5-SAIN and Ad5-CMV (Ctrl) at the indicated MOIs for 12 to 16 h at 37°C and grown in medium containing heat-inactivated serum (2%) for 48 h. Following infection, the cells were serum starved (16 h), incubated in the absence (basal) or presence of insulin (100 ng/ml) for 30 min, lysed, and subjected to immunoprecipitation with antibodies to IRS-1. The washed immunoprecipitates were assayed for PI 3-K activity with PI as substrate, and the labeled PI 3-phosphate product (PI-3P) was resolved by thin-layer chromatography and visualized by autoradiography. The experiment was repeated five times with similar results and a representative experiment is shown.

activation and glucose transport in differentiated 3T3-L1 adipocytes, despite the fact that IRS-1-associated PI 3-K and $p70^{s6k}$ are inhibited. We have previously shown that Shc and the downstream elements of the ras-MAPK pathway are not important signalling molecules for insulin stimulation of glucose transport (13). On the other hand, it has been suggested that IRS-1 is a key and necessary molecule mediating this important metabolic effect of insulin (4, 28, 48).

Our findings on 2-DOG uptake in 3T3-L1 adipocytes indicate that inhibition of IRS-1 phosphorylation and its associated PI 3-K activity due to disruption of IRS-1–IR interactions does not alter insulin-mediated glucose transport. Although it has been postulated that IRS-1, which is a major substrate of the insulin receptor, is a key signalling molecule in insulin stimulation of glucose transport, our data indicate that this may not be the case or, at least, that IRS-1 is not an absolute requirement for signalling of this major metabolic effect. Three recent studies have provided evidence consistent with our findings. For example, two groups independently have generated IRS-1 gene knockout mice which, surprisingly, are not diabetic and exhibit only minor defects in their ability to respond to insulin and regulate blood glucose levels (1, 43). In addition, Quon et al. (34) have shown that antisense ablation of IRS-1 mRNA has only a modest effect on the insulin sensitivity of GLUT4 translocation in primary adipocytes and has no effect on GLUT4 translocation at maximal insulin concentrations. A similar report from our laboratory showed that microinjection of IRS-1 blocking reagents did not inhibit stimulation of GLUT4 translocation (26), suggesting that IRS-1 is not essential for this effect.

Further studies of the IRS-1 knockout mice revealed that IRS-2, a molecule very similar to IRS-1, is phosphorylated by the IR and may compensate for the lack of IRS-1 (31). Thus, it is reasonable to ask whether signalling through IRS-2 is the reason we were unable to inhibit 2-DOG uptake by overexpression of the IRS-1-blocking PTB and SAIN proteins. We believe this is unlikely. Since the PTB domains of IRS-1 and IRS-2 are highly homologous (42), IRS-2 function should also be blocked by overexpression of the IRS-1 PTB domain. This is supported by the data in Fig. 2A and 6 which show marked inhibition of phosphorylation of the 180- to 190-kDa protein in PTB- and SAIN-expressing 3T3-L1 cells, since this region includes IRS-2 as well as IRS-1.

Several lines of evidence suggest that PI 3-K is a necessary molecule for insulin stimulation of glucose transport (2, 5, 7, 13, 29). Phosphorylated IRS-1 binds to the SH2 domains of the p85 subunit of PI 3-K, which in turn binds to and activates its p110 subunit, and this is a major mechanism by which insulin stimulates this enzyme. However, since inhibition of IRS-1 phosphorylation did not inhibit glucose transport, this suggests the presence of a separate, or redundant, pathway sufficient to connect the IR to activation of PI 3-K when IRS-1 is inhibited. Although we observed a substantial inhibition of IRS-1-associated PI 3-K activity due to PTB and SAIN protein overexpression, we did not find any effect of this on glucose transport stimulation. In this regard, it is important to point out that IRS-1-associated PI 3-K activity represents only a fraction of total cellular PI 3-K activity (22, 23, 46), and therefore, it seems possible that there are other means to connect the IR to PI 3-K activity which do not involve phosphorylated IRS-1. Along these lines, it has been shown that the IR can directly activate PI 3-K by binding to the p85 subunit through a phosphotyrosine motif in the insulin receptor C terminus (23, 46). Possibly this mechanism provides sufficient PI 3-K activation for stimulation of glucose transport, but not for other insulin bioeffects, particularly when IRS-1 function is inhibited. Indeed, we have found that a small fraction (<5%) of insulin-stimulated PI 3-K activity is associated with the IR, as measured by PI 3-K activity in IR immunoprecipitates, and the amount of this receptor-associated PI 3-K activity was somewhat increased in the PTB- and SAIN-expressing cells. Furthermore, there may be additional, unrecognized molecules that transduce signals from the IR to regulate glucose transport. For example, a new IRS-1-like molecule, termed Gab1, has recently been cloned and been shown to couple the IR to PI 3-K activation (15). The biologic function of Gab1 remains

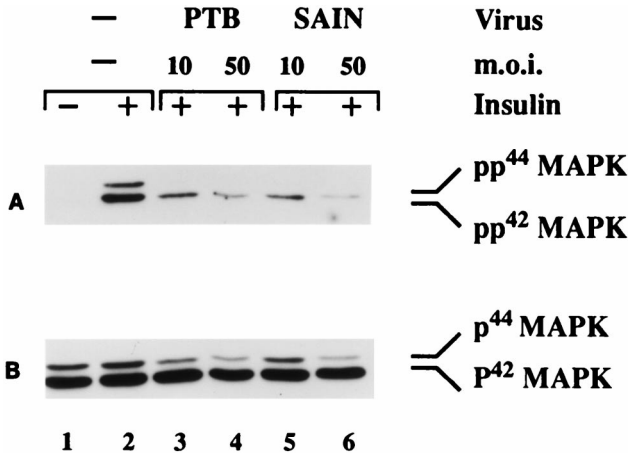

FIG. 8. Effects of overexpression of the Ad5-PTB and Ad5-SAIN domains on insulin-stimulated MAPK phosphorylation and expression in 3T3-L1 adipocytes. Cells were infected with Ad5-PTB- and Ad5-SAIN-expressing adenoviruses at the indicated MOIs in medium containing heat-inactivated serum (2%) for 12 to 16 h. Following infection, cells were serum starved (16 h), incubated in the absence (basal) or presence of insulin (100 ng/ml) for 5 min, lysed, subjected to SDS-PAGE, and immunoblotted with phosphospecific MAPK antibody (A). This experiment was repeated twice. To detect the levels of expression of p44 and p42 MAPK, the above-described filter was stripped and reblotted with anti-ERK1 antibody. There was no significant difference in the levels of expression between uninfected and infected 3T3-L1 adipocytes (B).

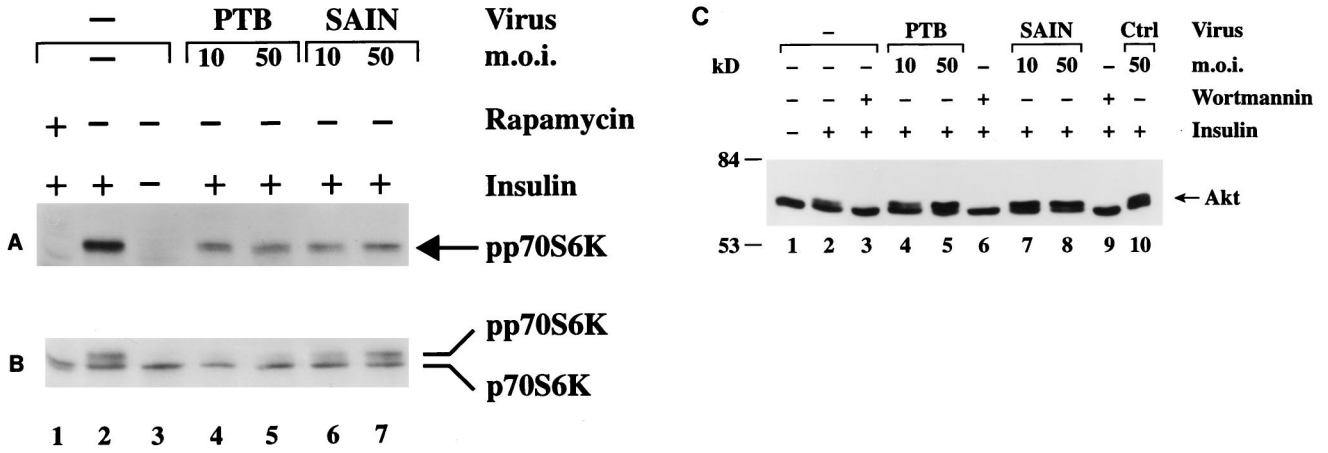

FIG. 9. Effects of overexpression of the PTB and SAIN domains on insulin-stimulated $p70^{s6k}$ activation in 3T3-L1 adipocytes. Cells were infected with Ad5-PTB- and Ad5-SAIN at the indicated MOIs for 12 to 16 h. Serum-starved (16 h) cells were incubated in the absence (basal) or presence of insulin (100 ng/ml) for 30 min, lysed, subjected to SDS-PAGE, and immunoblotted with phospho-specific $p70^{s6k}$ antibody (A). Filters were then stripped and reblotted with $p70^{s6k}$ antibody (B). Insulin stimulation of serine-threonine phosphorylation of $p70^{s6k}$ was detected by a retarded migration of the enzyme (panel B, lane 2). (C) Effects of overexpression of the PTB and SAIN domains on insulin-stimulated AKT activation in 3T3-L1 adipocytes. Whole-cell lysates (60 μg) were prepared as described above for panel A and were subjected to SDS-PAGE and immunoblotted with AKT antibody. Insulin stimulation of serine and threonine phosphorylation of AKT was detected by a retarded migration of the enzyme (lane 2). Preincubation with 100 nM wortmannin for 30 min inhibited activation of AKT (lanes 3, 6, and 9). Overexpression of either PTB (lanes 4 and 5) or SAIN (lanes 7 and 8) did not affect AKT activation. This experiment was repeated four times.

to be elucidated. Lastly, other substrates of the IR have recently been identified (22, 25, 50, 52), and subsequent studies may indicate a role for these new substrates in insulin's metabolic effects.

Our data show that in 3T3-L1 adipocytes, some downstream targets of PI 3-K, such as $p70^{s6k}$ (5), are inhibited by blocking IRS-1-associated PI 3-K activity, whereas other downstream targets of PI 3-Kinase, i.e., AKT (9) and glucose transport (7), are not. We also find that AKT phosphorylation and glucose transport stimulation are both inhibitable by wortmannin. This leads to the new conclusion that there is a bifurcation in the insulin signalling pathway, at least in 3T3-L1 adipocytes, such that while AKT and glucose transport are downstream of PI 3-K, they do not need to be dependent on IRS-1-associated PI

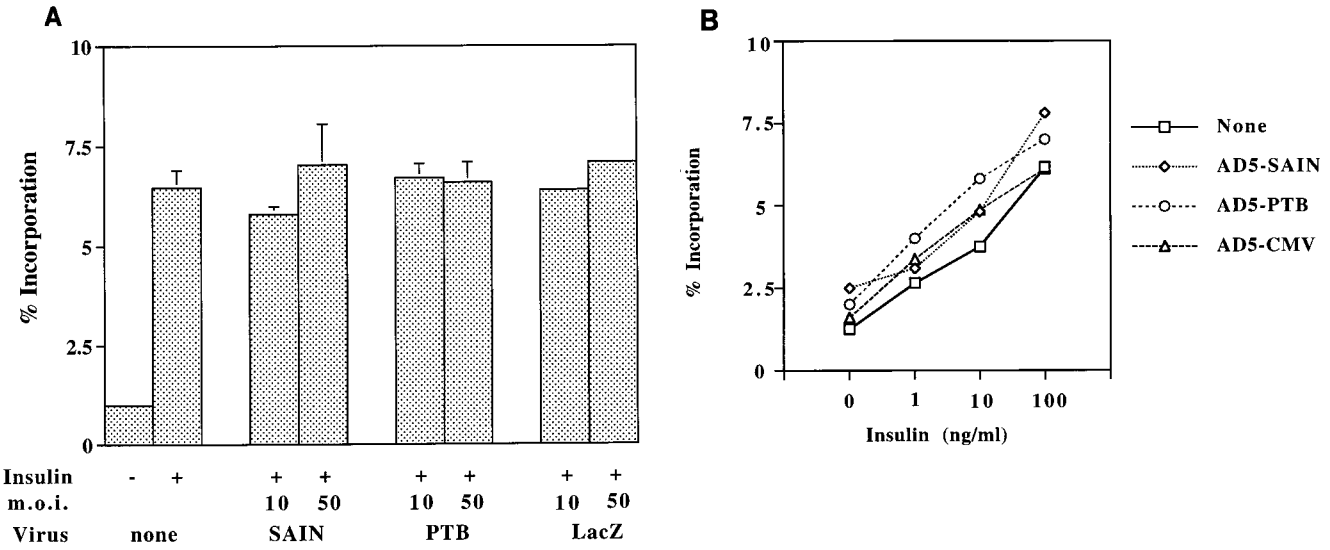

FIG. 10. (A) 2-DOG transport in 3T3-L1 adipocytes infected with increasing MOIs of adenoviruses expressing PTB and SAIN domains of IRS-1. Differentiated 3T3-L1 adipocytes were infected with Ad5-PTB, Ad5-SAIN, or Ad5-lacZ at the indicated MOIs for 12 to 16 h at 37°C or were not infected and were grown in medium containing heat-inactivated serum (2%) for 48 h. Serum- and glucose-deprived cells were incubated in α-MEM in the absence (basal) or presence of 100 ng of insulin/ml for 1 h at 37°C. Cells were then washed with glucose-free medium, and 2-DOG uptake was measured. Each measurement was performed in duplicate. Infection of differentiated 3T3-L1 adipocytes with Ad5-PTB and Ad5-SAIN did not affect the insulin-stimulated percent incorporation of 2-DOG transport. Control Ad5-lacZ virus had no effect on glucose transport. Data are representative of three different observations and each value was corrected for total cellular protein content. Each value represents the mean ± standard error of the mean of three experiments. (B) 2-DOG transport in 3T3L-1 adipocytes as a function of insulin concentration. Differentiated 3T3-L1 adipocytes were infected with Ad5-PTB, Ad5-SAIN, or Ad5-CMV at an MOI of 50 for 12 to 16 h at 37°C or were not infected and were grown in medium containing heat-inactivated serum (2%) for 48 h. Serum- and glucose-deprived cells were incubated in α-MEM in the absence (basal) or presence of 1, 10, and 100 ng of insulin/ml for 1 h at 37°C. Cells were then washed in glucose-free medium, and 2-DOG uptake was measured. Each measurement was performed in duplicate. Insulin stimulated the percent incorporation of 2-DOG in 3T3-L1 adipocytes in a dose-dependent manner, which was not altered by overexpression of either the PTB or the SAIN protein. Control Ad5 virus (Ad5-CMV) had no effect on glucose transport. Data are representative of three different observations.

3-K. On the other hand, $p70^{s6k}$ activation is dependent on IRS-1-associated PI 3-K activity. Thus, the insulin signal must be able to stimulate a component of PI 3-K through a mechanism independent of IRS-1 (or IRS-2), and this stimulated PI 3-K is sufficient to activate AKT and glucose transport. In addition, our findings further tighten the connection of AKT as an upstream activator of GLUT4 translocation (21). Finally, since $p70^{s6k}$ is inhibited in the absence of a decrease in AKT phosphorylation, these findings would indicate that, in these cells, AKT activation is not sufficient for $p70^{s6k}$ stimulation and that some additional input from the insulin action pathway to $p70^{s6k}$ which traverses IRS-1–PI 3K must be necessary.

Another interpretation of our data is that the dose responses for DNA synthesis, activation of PI 3-K, MAPK, $p70^{s6k}$, and AKT, and glucose transport are quantitatively different. Thus, perhaps only a small amount of IRS-1 is necessary to mediate AKT activation and subsequent glucose transport, and since the overexpressed PTB and SAIN domains do not totally inhibit IRS-1 phosphorylation, any remaining functional IRS-1 might be sufficient to allow glucose transport to occur. In this event, however, one would expect that at submaximally effective insulin concentrations, the amount of phosphorylated IRS-1 should be rate limiting for stimulation of glucose transport. Our data show that at insulin concentrations which only stimulate 50% of maximal glucose transport, overexpression of the PTB and SAIN proteins still does not inhibit this effect of insulin. Lastly, one might speculate that while IRS-1 is normally involved in coupling the IR to AKT activation, leading to stimulation of glucose transport, when IRS-1 is inhibited, a preexisting, redundant, signalling pathway can take over this function. Such a sequence of events would still mean that IRS-1 is not absolutely necessary for this biologic action of insulin, and it would be important to identify the molecular components of this putative redundant pathway.

ACKNOWLEDGMENTS

This work was funded by NIH research grant R01 DK 36651 to J.M.O. K.E. was supported by the Uehara Memorial Foundation. J.L.M. was supported by NIH training grant T32 DK 07202.

We thank Christopher B. Newgard for providing the adenovirus plasmids, Steven E. Shoelson for providing human IRS-1 cDNA, and James G. Nelson for providing differentiated 3T3-L1 adipocytes. We also thank Aron Morris, Dorothy Sears, Nick Webster, Theodore P. Ciaraldi, T. S. Pillay, William A. Ricketts, and Wolfgang Dillman for many helpful discussions, suggestions, and critical comments.

REFERENCES

1. **Araki, E., M. A. Lipes, M.-E. Patti, J. C. Bruning, B. Haag III, R. S. Johnson, and C. R. Kahn.** 1994. Alternative pathway of insulin signalling in mice with targeted disruption of the IRS-1 gene. Nature **372:**186–190.
2. **Backer, J. M., M. G. Myers, Jr., X.-J. Sun, D. J. Chin, S. E. Shoelson, M. Miralpeix, and M. F. White.** 1993. Association of IRS-1 with the insulin receptor and the phosphatidylinositol 3′-kinase. J. Biol. Chem. **268:**8204–8212.
3. **Blaikie, P., D. Immanuel, J. Wu, N. Li, V. Yajnik, and B. Margolis.** 1994. A region in Shc distinct from the SH2 domain can bind tyrosine-phosphorylated growth factor receptors. J. Biol. Chem. **269:**32031–32034.
4. **Cheatham, B., and C. R. Kahn.** 1995. Insulin action and the insulin signalling network. Endocr. Rev. **16:**117–142.
5. **Cheatham, B., C. J. Vlahos, L. Cheatham, L. Wang, J. Blenis, and C. R. Kahn.** 1994. Phosphatidylinositol 3-kinase activation is required for insulin stimulation of pp70 S6 kinase, DNA synthesis, and glucose transporter translocation. Mol. Cell. Biol. **14:**4902–4911.
6. **Chung, J., C. J. Kuo, G. R. Crabtree, and J. Blenis.** 1992. Rapamycin-FKBP specifically blocks growth-dependent activation of and signalling by the 70 kd S6 protein kinsase. Cell **69:**1227–1236.
7. **Clarke, J. F., P. W. Young, K. Yonezawa, M. Kasuga, and G. D. Holman.** 1994. Inhibition of translocation of GLUT1 and GLUT4 in 3T3-L1 cells by the phosphatidylinositol 3-kinase inhibitor, wortmannin. Biochem. J. **300:**631–635.
8. **Craparo, A., T. J. O'Neill, and T. A. Gustafson.** 1995. Non-SH2 domains within insulin receptor substrate-1 and SHC mediate their phosphotyrosine-dependent interaction with the NPEY motif of the insulin-like growth factor 1 receptor. J. Biol. Chem. **270:**15639–15643.
9. **Datta, K., A. Bellacosa, T. O. Chan, and P. N. Tsichlis.** 1996. Akt is a direct target of the phosphatidylinositol 3-kinase. J. Biol. Chem. **271:**30835–30839.
10. **Eck, M. J., S. Dhe-Paganon, T. Trub, R. T. Nolte, and S. E. Shoelson.** 1996. Structure of the IRS-1 PTB domain bound to the juxtamembrane region of the insulin receptor. Cell **85:**695–705.
11. **Gluzman, Y., H. Reichl, and D. Solnick.** 1982. Helper-free adenovirus type-5 vectors, p. 187–192. *In* Y. Gluzman (ed.), Eucaryotic viral vectors, Cold Spring Harbor Laboratory, Cold Spring Harbor, N.Y.
12. **Gustafson, T. A., W. He, A. Craparo, C. D. Schaub, and T. J. O'Neill.** 1995. Phosphotyrosine-dependent interaction of SHC and insulin receptor substrate 1 with the NPEY motif of the insulin receptor via a novel non-SH2 domain. Mol. Cell. Biol. **15:**2500–2508.
13. **Haruta, T., A. J. Morris, D. W. Rose, J. G. Nelson, M. Mueckler, and J. M. Olefsky.** 1995. Insulin-stimulated GLUT4 translocation is mediated by a divergent intracellular signalling pathway. J. Biol. Chem. **270:**27991–27994.
14. **He, W., T. J. O'Neill, and T. A. Gustafson.** 1995. Distinct modes of interaction of SHC and insulin receptor substrate-1 with the insulin receptor NPEY region via non-SH2 domains. J. Biol. Chem. **270:**23258–23262.
15. **Holgado-Madruga, M., D. R. Emlet, D. K. Moscatello, A. K. Godwin, and A. J. Wong.** 1996. A Grb2-associated docking protein in EGF- and insulin-receptor signalling. Nature **379:**560–564.
16. **Isakoff, S. J., Y.-P. Yu, Y.-C. Su, P. Blaikie, V. Yajnik, E. Rose, K. M. Weidner, M. Sachs, B. Margolis, and E. Y. Skolnik.** 1996. Interaction between the phosphotyrosine binding domain of Shc and the insulin receptor is required for Shc phosphorylation by insulin in vivo. J. Biol. Chem. **271:**3959–3962.
17. **Jhun, B. H., D. W. Rose, B. L. Seely, L. Rameh, L. Cantley, A. R. Saltiel, and J. M. Olefsky.** 1994. Microinjection of the SH2 domain of the 85-kilodalton subunit of phosphatidylinositol 3-kinase inhibits insulin-induced DNA synthesis and c-*fos* expression. Mol. Cell. Biol. **14:**7466–7475.
18. **Kavanaugh, W. M., and L. T. Williams.** 1994. An alternative to SH2 domains for binding tyrosine-phosphorylated proteins. Science **266:**1862–1865.
19. **Klip, A., G. Li, and W. J. Logan.** 1984. Induction of sugar uptake in response to insulin by serum depletion in fusing L6 myoblasts. Am. J. Physiol. **247:**E291–E296.
20. **Kohn, A. D., K. S. Kovacina, and R. A. Roth.** 1995. Insulin stimulates the kinase activity of RAC-PK, a pleckstrin homology domain containing ser/thr kinase. EMBO J. **14:**4288–4295.
21. **Kohn, A. D., S. A. Summers, M. J. Birnbaum, and R. A. Roth.** 1996. Expression of a constitutively active Akt Ser/Thr kinase in 3T3-L1 adipocytes stimulates glucose uptake and glucose transporter 4 translocation. J. Biol. Chem. **271:**31372–31378.
22. **Lavan, B. E., and G. E. Lienhard.** 1993. The insulin-elicited 60-kDa phosphotyrosine protein in rat adipocytes is associated with phosphatidylinositol 3-kinase. J. Biol. Chem. **268:**5921–5928.
23. **Levy-Toledano, R., M. Taouis, D. H. Blaettler, P. Gorden, and S. I. Taylor.** 1994. Insulin-induced activation of phosphatidyl inositol 3-kinase. J. Biol. Chem. **269:**31178–31182.
24. **McGrory, W. J., D. S. Bautista, and F. L. Graham.** 1988. A simple technique for the rescue of early region I mutations into infectious human adenovirus type 5. Virology **163:**614–617.
25. **Momomura, K., K. Tobe, Y. Seyama, F. Takaku, and M. Kasuga.** 1988. Insulin-induced tyrosine-phosphorylation in intact rat adipocytes. Biochem. Biophys. Res. Commun. **155:**1181–1186.
26. **Morris, A. J., S. S. Martin, T. Haruta, J. G. Nelson, P. Vollenweider, T. A. Gustafson, M. Mueckler, D. W. Rose, and J. M. Olefsky.** 1996. Evidence for an insulin receptor substrate 1 independent insulin signalling pathway that mediates insulin-responsive glucose transporter (GLUT4) translocation. Proc. Natl. Acad. Sci. USA **93:**8401–8406.
27. **Myers, M. G., Jr., T. C. Grammer, J. Brooks, E. M. Glasheen, L.-M. Wang, X. J. Sun, J. Blenis, J. H. Pierce, and M. F. White.** 1995. The pleckstrin homology domain in insulin receptor substrate-1 sensitizes insulin signalling. J. Biol. Chem. **270:**11715–11718.
28. **Myers, M. G., Jr., and M. F. White.** 1995. New frontiers in insulin receptor substrate signalling. Trends Endocrinol. Metab. **6:**209–215.
29. **Okada, T., Y. Kawano, T. Sakakibara, O. Hazeki, and M. Ui.** 1994. Essential role of phosphatidylinositol 3-kinase in insulin-induced glucose transport and antilipolysis in rat adipocytes. J. Biol. Chem. **269:**3568–3573.
30. **Ouwens, D. M., G. C. M. van der Zon, G. J. Pronk, J. L. Bos, W. Moller, B. Cheatham, C. R. Khan, and J. A. Maassen.** 1994. A mutant insulin receptor induces formation of a Shc-growth factor receptor bound protein 2 (Grb2) complex and p21ras-GTP without detectable interaction of insulin receptor substrate 1 (IRS1) with Grb2. J. Biol. Chem. **269:**33116–33122.
31. **Patti, M.-E., X.-J. Sun, J. C. Bruening, E. Araki, M. A. Lipes, M. F. White, and C. R. Kahn.** 1995. 4PS/insulin receptor substrate (IRS)-2 is the alternative substrate of the insulin receptor in IRS-1 deficient mice. J. Biol. Chem. **270:**24670–24673.
32. **Pronk, G. J., J. McGlade, G. Pelicci, T. Pawson, and J. L. Bos.** 1993.

Insulin-induced phosphorylation of the p46- and 52-kDa Shc proteins. J. Biol. Chem. **268:**5748–5753.
33. **Pronk, G. J., A. M. M. De Vries-Smits, L. Buday, J. Downward, J. A. Maassen, R. H. Medema, and J. L. Bos.** 1994. Involvement of Shc in insulin- and epidermal growth factor-induced activation of p21ras. Mol. Cell. Biol. **14:**1575–1581.
34. **Quon, M. J., A. J. Butte, M. J. Zarnowski, G. Sesti, S. W. Cushman, and S. I. Taylor.** 1994. Insulin receptor substrate 1 mediates the stimulatory effect of insulin on GLUT4 translocation in transfected rat adipose cells. J. Biol. Chem. **269:**27920–27924.
35. **Rose, D. W., A. R. Saltiel, M. Majumdar, S. J. Decker, and J. M. Olefsky.** 1994. Insulin receptor substrate 1 is required for insulin-mediated mitogenic signal transduction. Proc. Natl. Acad. Sci. USA **91:**797–801.
36. **Ruderman, N. B., R. Kapeller, M. F. White, and L. C. Cantley.** 1990. Activation of phosphatidylinositol 3-kinase by insulin. Proc. Natl. Acad., Sci. USA **87:**1411–1415.
37. **Sasaoka, T., B. Draznin, J. W. Leitner, W. J. Langlois, and J. M. Olefsky.** 1994. Shc is the predominant signalling molecule coupling insulin receptors to activation of guanine nucleotide releasing factor and p21ras-GTP formation. J. Biol. Chem. **269:**10734–10738.
38. **Sharma, P. M., M. Bowman, B.-F. Yu, and S. Sukumar.** 1994. An animal model for human Wilm's tumors: embryonal kidney neoplasms in rats induced by *N*-nitroso-*N*′-methyl urea. Proc. Natl. Acad. Sci. USA **91:**9931–9935.
39. **Skolnik, E. Y., A. Batzer, N. Li, C.-H. Lee, E. Lowenstein, M. Mohammadi, B. Margolis, and J. Schlessinger.** 1993. The function of GRB2 in linking the insulin receptor to Ras signalling pathways. Science **260:**1953–1955.
40. **Skolnik, E. Y., C.-H. Lee, A. Batzer, L. M. Vicentini, M. Zhou, R. Daly, M. J. Myers, Jr., J. M. Backer, A. Ullrich, M. F. White, and J. Schlessinger.** 1993. The SH2/SH3 domain-containing protein GRB2 interacts with tyrosine-phosphorylated IRS1 and Shc: implications for insulin control of ras signalling. EMBO J. **12:**1929–1936.
41. **Sun, X. J., P. Rothenberg, C. R. Kahn, J. M. Backer, E. Araki, P. A. Wilden, D. A. Cahill, B. J. Goldstein, and M. F. White.** 1991. Structure of the insulin receptor substrate IRS-1 defines a unique signal transduction protein. Nature **352:**73–77.
42. **Sun, X. J., L.-M. Wang, Y. Zhang, L. Yenush, M. G. Myers, Jr., E. Glasheen, W. S. Lane, J. H. Pierce, and M. F. White.** 1995. Role of IRS-2 in insulin and cytokine signalling. Nature **377:**173–177.
43. **Tamemoto, H., T. Kadowaki, K. Tobe, T. Yagi, H. Sakura, T. Hayakawa, Y. Terauchi, K. Ueki, Y. Kaburagi, S. Satoh, H. Sekihara, S. Yoshioka, H. Horikoshi, Y. Furuta, Y. Ikawa, M. Kasuga, Y. Yazaki, and S. Aizawa.** 1994. Insulin resistance and growth retardation in mice lacking insulin receptor substrate-1. Nature **372:**182–186.
44. **Tartare-Deckert, S., D. Sawka-Verhelle, J. Murdaca, and E. V. Obberghen.** 1995. Evidence for a differential interaction of SHC and the insulin receptor substrate-1 (IRS-1) with the insulin-like growth factor-1 (IGF-1) receptor in the yeast two-hybrid system. J. Biol. Chem. **270:**23456–23460.
45. **Tobe, K., H. Tamemoto, T. Yamauchi, S. Aizawa, Y. Yazaki, and T. Kadowaki.** 1995. Identification of a 190-kDa protein as a novel substrate for the insulin receptor kinase functionally similar to insulin receptor substrate-1. J. Biol. Chem. **270:**5698–5701.
46. **Van Horn, D. J., M. G. Myers, Jr., and J. M. Backer.** 1994. Direct activation of the phosphatidylinositol 3′-kinase by the insulin receptor. J. Biol. Chem. **269:**29–32.
47. **Voliovitch, H., D. G. Schindler, Y. R. Hadari, S. I. Taylor, D. Accili, and Y. Zick.** 1995. Tyrosine phosphorylation of insulin receptor substrate-1 *in vivo* depends upon the presence of its pleckstrin homology region. J. Biol. Chem. **270:**18083–18087.
48. **Waters, S. B., and J. E. Pessin.** 1996. Insulin receptor substrate 1 and 2 (IRS1 and IRS2): what a tangled web we weave. Trends Cell. Biol. **6:**1–4.
49. **White, M. F., R. Maron, and C. R. Kahn.** 1985. Insulin rapidly stimulates tyrosine phosphorylation of a Mr-185,000 protein in intact cells. Nature **318:**183–186.
50. **Yeh, T. C., W. Ogawa, A. G. Danielsen, and R. A. Roth.** 1996. Characterization and cloning of a 58/53-kDa substrate of the insulin receptor tyrosine kinase. J. Biol. Chem. **271:**2921–2928.
51. **Zhang, W.-W., P. E. Koch, and J. A. Roth.** 1995. Detection of wild-type contamination in a recombinant adenoviral preparation by PCR. Biotechniques **18:**444–447.
52. **Zhang-Sun, G., C.-R. Yang, J. Viallet, G.-S. Feng, J. J. M. Bergeron, and B. I. Posner.** 1996. A 60-kilodalton protein in rat hepatoma cells overexpressing insulin receptor was tyrosine phosphorylated and associated with Syp, phosphatidylinositol 3-kinase, and Grb2 in an insulin-dependent manner. Endocrinology **137:**2649–2658.